Correlation-Based Sensing for Cognitive Radio Networks: Bounds and Experimental Assessment

Rajesh K. Sharma, *Student Member, IEEE*, and Jon W. Wallace, *Member, IEEE*

***Abstract*—Minimal missed detection rate of primary users is critical for adoption of cognitive radio networks, underlining the need for robust collaborative sensing combined with near-optimal single-node detection methods. Although correlation-based detection methods potentially provide needed per-node performance improvements for correlated signals, their performance for realistic blind sensing is unclear since the type and extent of correlation may be unknown in practice. Although standard Neymon–Pearson (NP) based detection can be applied when correlation is perfectly known, difficulty arises when the correlation is random, which is the focus of this paper. A tighter bound for the performance of correlation-based methods is developed herein based on a signal with random correlation and NP detection under the assumption of correlation distribution information (CDI). Simulations of existing ad-hoc correlation-based detectors are compared to the upperbound using a simple uniform random correlation model (RCM). Additionally, a measurement campaign is presented where radio-frequency (RF) spectra in many bands of interest are measured throughout a large sub-urban environment, generating realistic models for the random signal correlation. The measurement-based model indicates limits on performance gains possible with correlation-based detection and how well existing ad-hoc techniques can be expected to perform in practice.**

***Index Terms*—Cognitive radio, correlation, Neyman–Pearson (NP) criterion, signal detection.**

I. Introduction

IT IS WELL recognized that possible adoption of cognitive radio [1] technologies that overlay existing licensed services will require extremely robust sensing with vanishing missed detection rates in order to incur negligible impact on primary users. An obstacle to robust sensing that is most problematic for simplex (broadcast) and frequency-division duplex (FDD) primary systems is the "hidden node" problem [2], where due to primary signal shadowing, the cognitive radio believes a primary transmitter is not present, and subsequent utilization of the band interferes with a primary receiver that is not shadowed. A promising solution for robust detection in the presence of hidden node is collaborative sensing or cooperative sensing, where sensor fusion is performed on information collected at multiple distributed cognitive nodes [3]–[5]. In this case, seemingly modest improvements in the per-node detection performance (10%–20%) can have dramatic impact on the missed-detection performance of the network, fueling interest in developing near-optimal detection methods at the cognitive nodes. Although energy detection (ED) [6]–[8] is a classical method that is typically used in practice for blind sensing, increased performance is possible by exploiting additional signal parameters.

The focus of this paper is correlation-based detection (CBD) methods for unknown (random) correlation that exploit potential signal autocorrelation arising from pilot tones, signal guardbands, partially occupied spectrum, frequency-selective propagation channels, etc., for improved detection performance. One ad-hoc CBD technique is the covariance absolute value (CAV) method [9], which exploits the sample covariance matrix to provide a constant false alarm rate detector. In [10], we presented analytical expressions for the performance of an alternative ad-hoc detector that exploits both energy and correlation (the CorrSum method), but the optimality of the detector was not considered and only theoretical results were presented without any experimental assessment. Although significant performance improvements are possible with the ad-hoc CBDs, a tight upperbound for these methods has been impeded by the dependence of detection rates on the actual nature and level of correlation present, which is unknown (random) in practice.

In this paper, we propose random correlation models (RCMs), where correlation is a random variable whose distribution can be exploited, allowing the performance of CBD methods to be precisely assessed. Although the optimal detector for known correlation is given by the well-known Neyman–Pearson (NP) detector, resulting in the estimator correlator [11], the performance of this detector provides only a loose upperbound for unknown correlation. To obtain a tighter upperbound on CBD performance, this work considers optimal NP detection when only the *parameters* of the RCM are known *a priori*, as opposed to knowing the *realizations* of the RCM that are required for a standard NP-based estimator-correlator. Two RCMs are considered in this work: (i) a simple uniform correlation model, appropriate when correlated signals are present, but the exact level is unknown and (ii) a realistic model based on actual radio-frequency (RF) spectrum measurements taken throughout the city of Bremen, Germany.

Before proceeding, we note that cyclostationary detection [12], [13] is a generalization of CBD methods, since the cyclic spectrum comprises the same information as the signal autocorrelation at the zero cyclic frequency shift. An advantage of cyclostationary detection is the ability to operate at very low SNR due to inherent immunity to noise uncertainty

Manuscript received May 14, 2010; accepted July 04, 2010. Date of publication September 23, 2010; date of current version January 26, 2011. The associate editor coordinating the review of this paper and approving it for publication was Dr. Subhas Mukhopadhyay.

The authors are with the School of Engineering and Science, Jacobs University Bremen, Campus Ring 1, 28759 Bremen, Germany (e-mail: ra.sharma@jacobs-university.de; wall@ieee.org).

Color versions of one or more of the figures in this paper are available online at http://ieeexplore.ieee.org.

Digital Object Identifier 10.1109/JSEN.2010.2058097

(NU) [14]. On the other hand, either *a priori* knowledge of modulation-specific peak locations in the cyclic spectrum or a scanning algorithm is required. Since performance depends on the type of signals present, the random cyclic spectrum must be modeled, which is even more complicated than the simple RCMs considered in this work. Furthermore, cyclostationary methods can have some practical issues, such as the need for very long observation times with high computational complexity [15], and ultrastable synchronization [14]. For these reasons, cyclostationary detection is not treated in this current work and is left as the subject of future investigations.

The remainder of this paper is organized as follows: Section II provides background on the system model, reviews energy detection, outlines two ad-hoc correlation-based detection methods (CAV and CorrSum) that are to be assessed, and ends with a concise example of collaborative sensing that motivates the search for near-optimal sensing methods. Optimal sensing is treated in Section III, where random correlation modeling allows NP detection with perfect correlation information (NP-PCI) to be generalized to the optimal detector with correlation distribution information (NP-CDI). A measurement campaign used to generate an RCM for a realistic sub-urban environment is presented in Section IV. Section V assesses the performance of existing ad-hoc CBD methods based on the developed RCMs in light of the NP bounds, and concluding remarks are given in Section VI.

II. System Model and Primary Signal Detection

This section provides the signal model and important results from detection theory that are needed for later analysis. Boldface lowercase and uppercase letters denote vectors and matrices, respectively. Vector transpose and conjugate transpose (Hermitian) are indicated by $\mathbf{x}^T$ and $\mathbf{x}^H$, respectively. The imaginary unit is indicated by j, and $|\cdot|$ and $\angle\cdot$ take the magnitude and phase of a complex argument. The notation $\mathbf{x} \sim \mathcal{Z}$ indicates that the random vector (or variable) $\mathbf{x}$ has the probability distribution $\mathcal{Z}$. The distribution $\mathcal{CN}(\boldsymbol{\mu}, \mathbf{R})$ is the multivariate complex Gaussian distribution with mean vector $\boldsymbol{\mu}$ and covariance matrix $\mathbf{R}$ having the corresponding probability density function (pdf)

$$p_{\mathrm{cn}}(\mathbf{x}|\mathbf{R}) = \frac{1}{\pi^N |\mathbf{R}|} \exp[-(\mathbf{x}-\boldsymbol{\mu})^H \mathbf{R}^{-1} (\mathbf{x}-\boldsymbol{\mu})] \quad (1)$$

where N is the length of $\mathbf{x}$ and $|\cdot|$ is determinant. $\mathcal{N}(\boldsymbol{\mu}, \mathbf{R})$ denotes the usual multivariate real Gaussian distribution with mean $\boldsymbol{\mu}$ and covariance $\mathbf{R}$, and $U(a,b)$ is the uniform distribution on the interval $[a,b]$. Additional notation will be introduced as necessary.

A. Signal Model

Considering a single cognitive radio node that samples received RF waveforms limited to bandwidth W by an ideal bandpass filter, the vector of complex baseband samples is $\mathbf{x} = \mathbf{x}_R + j\mathbf{x}_I$, where $\mathbf{x}_R$ and $\mathbf{x}_I$ are the real (in-phase) and imaginary (quadrature) components, respectively, each having bandwidth $W/2$. Further, we assume that efficient Nyquist sampling is employed, or that the sample frequency $f_s = W$, such that for sensing time T, $N = TW$ complex baseband samples are collected.

Receiver noise is modeled as a vector of complex Gaussian random samples $\mathbf{n}$, having a flat power spectral density (PSD) N_0 in the baseband sensing bandwidth. When Nyquist sampling is employed, noise samples are uncorrelated, since the autocorrelation for sample lag k is

$$\phi_{n,k} = \mathrm{E}\{n_i n_{i-k}^*\} = WN_0 \,\mathrm{sinc}(k) = \sigma_n^2 \delta[k] \quad (2)$$

where $\mathrm{sinc}(x) = \sin(\pi x)/(\pi x)$, total noise variance is $\sigma_n^2 = WN_0$, $\delta[k]$ is the Kronecker delta function, and the last equality comes since k is an integer. Thus, when only noise is present (referred to as hypothesis H_0) we have $\mathbf{x} = \mathbf{n} \sim \mathcal{CN}(0, \sigma_n^2 \mathbf{I})$, and the pdf for this case is denoted $p(\mathbf{x}; \mathsf{H}_0)$.

When signal is present (hypothesis H_1), the receiver measures signal plus noise $\mathbf{x} = \mathbf{s} + \mathbf{n}$, where $\mathbf{s}$ is a vector of signal samples confined to bandwidth W having autocorrelation $\phi_{s,k} = \mathrm{E}\{s_i s_{i-k}^*\}$. The correlation-based detectors studied in this work exploit the fact that $\phi_{s,k}$ can differ significantly from $\phi_{n,k}$. Normalized autocorrelation will be denoted $\rho_{r,k} = \phi_{r,k}/\phi_{r,0}$ with $r \in \{x, n, s\}$. The pdf of $\mathbf{x}$ for the case of signal present is denoted $p(\mathbf{x}; \mathsf{H}_1)$.

B. Primary Signal Detection

The optimal NP detector [11] forms the likelihood ratio

$$\mathcal{L}(\mathbf{x}) = \frac{p(\mathbf{x}; \mathsf{H}_1)}{p(\mathbf{x}; \mathsf{H}_0)} \quad (3)$$

and compares to a threshold λ, declaring H_1 (signal present) if $\mathcal{L}(\mathbf{x}) > \lambda$ and H_0 (noise only) otherwise. Probability of false alarm (P_{fa}) and probability of detection (P_d) are defined as

$$P_{fa} = \Pr\{\mathcal{L}(\mathbf{x}) > \lambda; \mathsf{H}_0\} = \int_{\{\mathbf{x}:\mathcal{L}(\mathbf{x})>\lambda\}} p(\mathbf{x}; \mathsf{H}_0)\, d\mathbf{x}, \quad (4)$$

$$P_d = \Pr\{\mathcal{L}(\mathbf{x}) > \lambda; \mathsf{H}_1\} = \int_{\{\mathbf{x}:\mathcal{L}(\mathbf{x})>\lambda\}} p(\mathbf{x}; \mathsf{H}_1)\, d\mathbf{x}. \quad (5)$$

The performance of detectors is routinely plotted in the form of receiver operating characteristics (ROCs) showing P_d versus P_{fa}. Note that NP detection is optimal in the sense of giving maximum P_d for an arbitrary fixed value of P_{fa}, and NP detectors will be applied in this work for the case of unknown (random) correlation. In the following, we discuss different correlation based detectors which are also summarized in Table I for convenience.

Energy detection (ED) performance will be considered as a base reference in this work, which operates by forming the test statistic $\mathcal{T}(\mathbf{x}) = \mathbf{x}^H\mathbf{x} = \mathbf{x}_R^T\mathbf{x}_R + \mathbf{x}_I^T\mathbf{x}_I$ and comparing this to a threshold λ. Under H_0, we have $\mathbf{x} = \mathbf{n}$ with the real and imaginary part of each sample having variance $\sigma_n^2/2$, meaning $2\mathcal{T}(\mathbf{x})/\sigma_n^2 \sim \chi_{2N}^2$, where χ_{2N}^2 is a central chi-squared distribution with $2N$ degrees of freedom.

Under H_1, there are two possible distributions for $\mathcal{T}(\mathbf{x})$ depending on the way $\mathbf{s}$ is modeled. In the first case, $\mathbf{s}$ is assumed to be a fixed (nonrandom) signal, leading to $\mathbf{x} \sim \mathcal{CN}(\mathbf{s}, \sigma_n^2\mathbf{I})$, such that $2\mathcal{T}(\mathbf{x})/\sigma_n^2$ is distributed as non-central chi-squared with $2N$ degrees of freedom and non-centrality parameter γ', denoted as $\chi_{2N}^2(\gamma')$, with $\gamma' = 2N\gamma$, where $\gamma = \mathbf{s}^H\mathbf{s}/(N\sigma_n^2)$

TABLE I
SUMMARY OF THE CONSIDERED DETECTION METHODS

Method	Exploiting Parameter	Required Knowledge	Features	Limitations	Analytical/Numerical Methods to Compute P_{fa}, P_d
ED	Energy	None	Simple	Suffers by NU	From [8], [10]
CorrSum	Energy and real 1st lag correlation	None	Simple, better detection than ED, less affected by NU	Ad-hoc, slightly more complex than ED	From [10] for fixed correlation, numerically using (15) for RCM
CAV	Covariance (absolute value)	None	Immune to NU	Ad-hoc, more complex than CorrSum, relatively poor performance without NU	From [9] for fixed correlation, numerically using (15) for RCM
NP-PCI	Covariance	Covariance	Optimal	May be impractical, only gives loose bound for CBD	Numerically from [11] for fixed correlation, numerically using (15) for RCM
NP-CDI	Covariance	Correlation distribution	Optimal, gives upper bound under CDI	Computationally complex	Pdfs of $\mathcal{T} = \mathcal{L}$ computed empirically with M Monte Carlo realizations of $\mathbf{x}$, with $\mathcal{T}$ computed numerically for each $\mathbf{x}$ using (10) in (3), followed by (13) and (14)

is the signal-to-noise ratio (SNR) [8]. In the second case, $\mathbf{s}$ is modeled as an uncorrelated zero-mean Gaussian random vector, meaning $\mathbf{x} \sim \mathcal{CN}(0, (\sigma_n^2 + \sigma_s^2)\mathbf{I})$, leading to $2\mathcal{T}(\mathbf{x})/(\sigma_n^2 + \sigma_s^2) \sim \chi^2_{2N}$ [11]. Probability of false alarm (4) and detection (5) for ED with a threshold λ can be computed in closed form [6], [8], [11], where numerical values of P_d are nearly identical for both signal models for sufficiently large N.

C. Ad-Hoc Correlation-Based Detectors

The performance of two existing ad-hoc correlation-based detectors will be assessed in this work: (i) the covariance absolute value (CAV) method and (ii) the correlation sum (CorrSum) method. Although expected to be suboptimal, both methods are attractive, since they have low complexity and require no *a priori* information about SNR or correlation.

The CAV method [9] forms a test statistic based on the absolute value of the receive covariance matrix $\mathbf{R}_x$ according to

$$\mathcal{T}(\mathbf{x}) = \frac{1}{\mathrm{Tr}\{\hat{\mathbf{R}}_x\}} \sum_{\ell=1}^{L} \sum_{m=1}^{L} |\hat{R}_{x,\ell m}| \tag{6}$$

where $\mathrm{Tr}\{\cdot\}$ is trace, and $\hat{\mathbf{R}}_x$ is the $L \times L$ sample covariance matrix $\hat{R}_{x,\ell m} = \hat{\phi}_{\ell - m}$ and $\hat{\phi}_k = (1/N)\sum_{i=1}^{N} x_i x_{i-k}^*$.

A feature of the CAV method is that normalization by the trace in (6) yields a test statistic under H_0 that is independent of the noise power, placing it in the class of constant false-alarm rate (CFAR) estimators [11]. In the case of NU [16], where accurate knowledge of σ_n^2 is not available, CFAR estimators can exhibit improved performance compared to their non-CFAR counterparts. Since the goal of this work is to develop near-optimal sensing methods, we mainly focus on the assumption where accurate noise estimates are available, but the case of NU is also considered briefly. The trace normalization in (6) unfortunately spreads the distribution of $\mathcal{T}(\mathbf{x})$, leading to seemingly poor performance when noise is known, but one should keep in mind that relative performance can change dramatically when NU is an issue.

A critical consideration in CAV is the choice of L (referred to as the smoothing factor in [9]), which can have a strong impact on the performance. No optimal choice for L is given in [9], likely because this depends on the level of correlation present, which is assumed to be unknown. One finding in our work is that for moderate correlation ($\rho_{s,1} \approx 0.5$), a value of $L = 2$ (exploiting only the first lag) yields the best performance, whereas larger values of L are only beneficial for high correlation. Although [9] requires that the receive noise be prewhitened, this operation is avoided in our analysis by assuming ideal filtering and Nyquist sampling at rate W, such that noise is always uncorrelated.

In [10] and [17], we proposed the simple correlation sum (CorrSum) detector that exploits both energy and correlation for improved performance, which forms the test statistic

$$\mathcal{T}(\mathbf{x}) = \hat{\phi}_{x,0} + \mathrm{Re}\{\hat{\phi}_{x,1}\} \tag{7}$$

which can be generalized to

$$\mathcal{T}(\mathbf{x}) = \sum_{i=0}^{L-1} \mathrm{Re}\{\hat{\phi}_{x,i}\} \tag{8}$$

for arbitrary maximum lag $L-1$.

Conceptually, the method measures deviation of the autocorrelation function from the noise-only case, whether this is due to increased energy or nonzero correlation, corresponding to the first and second terms in (7), respectively. Closed-form expressions for the performance of CorrSum are available in [10] for the Gaussian (large N) approximation on $\mathcal{T}(\mathbf{x})$.

For a signal with nearly real correlation (symmetric PSD), CorrSum can outperform CAV for two reasons: (i) For limited sample size, both real and imaginary parts of the noise autocorrelation $\hat{\phi}_{n,1}$ are nonzero. Since signal autocorrelation is known to be real, discarding useless information in the imaginary part of $\hat{\phi}_{x,1}$ is beneficial. (ii) Under H_0 and limited sample size, the real noise autocorrelation is positive or negative, yet the absolute value in CAV forces this to always be positive, causing more overlap of $p(\mathcal{T}; \mathsf{H}_0)$ and $p(\mathcal{T}; \mathsf{H}_1)$ and reducing potential performance.

On the other hand, when the signal PSD is not symmetric, $\hat{\phi}_s$ will be complex, and only exploiting the real autocorrelation discards useful information in the imaginary part, reducing detection performance. However, deviation from real autocorrelation due to a small frequency offset has negligible performance impact. Frequency offset is modeled by considering RF transmit signal centered at f_0, or $\mathrm{Re}\{s(t)\exp(j2\pi f_0 t)\}$, where translation to complex baseband using a different frequency f_0' and Nyquist sampling leads to a discrete signal $s_k' = s(k/W)\exp(j2\pi k \Delta f/W)$, where $\Delta f = f_0 - f_0'$. Although the $\exp(\cdot)$ term (offset) has no impact

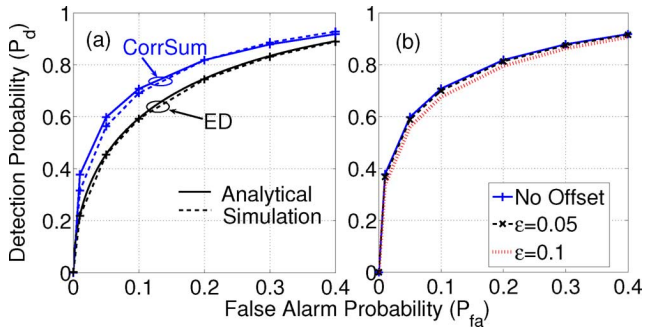

Fig. 1. ROC performance curves for ED and CorrSum methods. (a) Analytical models compared with Monte Carlo simulations. (b) Effect of carrier offset on CorrSum where $\varepsilon = \Delta f/W$.

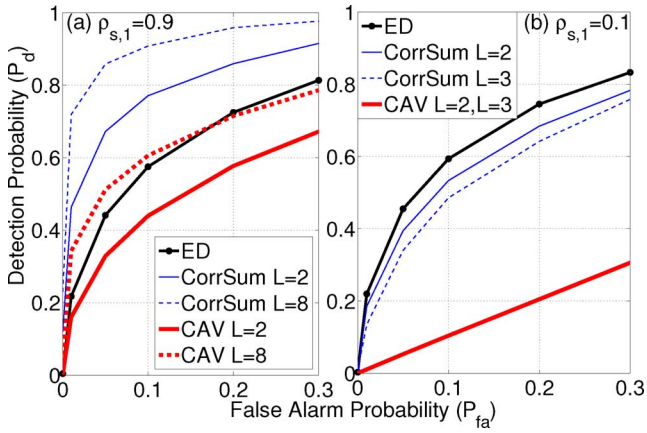

Fig. 2. Performance of ED, CorrSum, and CAV for (a) high correlation and (b) low correlation.

on the energy, the first-lag modified signal autocorrelation is $\rho'_{s,1} = \rho_{s,1}\exp(j2\pi\Delta f/W)$. Even assuming that the original spectrum is symmetric ($\rho_{s,1}$ positive real), the frequency offset leads to a small phase rotation in the complex plane.

In all numerical examples, we take $N = 160$ samples and SNR $\gamma = -9\,\mathrm{dB}$ for static channels or average SNR $\overline{\gamma} = -9\,\mathrm{dB}$ for fading channels. Fig. 1(a) compares ROC curves for ED and CorrSum methods using Monte Carlo simulations, as well as closed-form expressions given by (5), (6), (35), (36), and (37) in [10] for exponential correlation ($\rho_k = \rho_{s,k} = \rho_1^k$) with $\rho_1 = \rho_{s,1} = 0.5$. This result shows the performance improvement possible with correlation-based methods and also confirms that our Monte Carlo framework is correct. Fig. 1(b) demonstrates the effect of nonzero phase due to frequency offset, indicating that small offsets have negligible impact on performance.

Fig. 2 demonstrates the sensing performance of CAV and CorrSum for real correlation (guided sensing) in the presence of high and low correlation and explores the effect of including more lags in the test statistic. For high correlation (left) CAV and CorrSum have similar and better performance, respectively, compared to ED, and including many lags is beneficial. For low correlation, the CBD methods have lower performance than ED, and using more lags ($L \geq 2$) is detrimental.

D. Collaborative Sensing Example

Collaborative sensing, where cognitive nodes communicate detection decisions to a fusion center that makes a global decision, provides highly robust sensing in the presence of hidden node and low SNR [3], [4]. Fig. 3 shows the detection performance of single-sensor and eight-sensor fusion using "OR" and "majority" rule [18] for ED compared to the optimal correlation-based NP-CDI detector assuming that the channel between each sensor node and fusion center (also termed reporting channel [4]) is error-free, achieved in practice by robust link budget and error control coding in the reporting channel. Fig. 3(a) and (b) plot ROC curves for an idealized AWGN channel with a uniform RCM and a more realistic Rayleigh-fading channel with an empirically measured RCM, respectively. Details required to obtain the plotted single-sensor performance curves, such as the definition of the optimal NP-CDI detector (Section III) and the experimental random correlation model (Section V), are treated later in the paper. Nonetheless, this example illustrates that the seemingly modest improvement possible with correlation-based methods can lead to order of magnitude reduction in the missed detection rate of the overall cognitive radio network for eight-sensor fusion, strongly suggesting that refinement of existing algorithms to provide modest performance improvements, such as what is possible with correlation-based methods, is well worth the effort.

III. Modeling and Optimal Detection for CBD Methods

As stated previously, a rigorous definition for the performance of correlation-based detectors has not yet appeared, since it depends on the level of correlation present, which is unknown *a priori*. In this section, we present a new random-correlation framework that allows the performance of ad-hoc correlation methods to be assessed. Also, the upperbound on the performance of correlation-based detectors is found by considering an NP detector with correlation distribution information (CDI).

A. Random Correlation Modeling

For zero-mean complex Gaussian signal with fixed covariance matrix $\mathbf{R}_s$, the pdf of $\mathbf{x}$ is given by

$$p(\mathbf{x}) = \begin{cases} p_{\mathrm{cn}}(\mathbf{x}|\sigma_n^2\mathbf{I}), & \text{under } \mathsf{H}_0 \\ p_{\mathrm{cn}}(\mathbf{x}|\sigma_n^2\mathbf{I}+\mathbf{R}_s), & \text{under } \mathsf{H}_1 \end{cases}. \tag{9}$$

Since signal correlation is not assumed to be known for correlation-based detectors, we model the random signal covariance as $\mathbf{R}_s(\mathbf{\Omega})$, where $\mathbf{\Omega}$ is a vector of random parameters, and $p(\mathbf{x})$ under H_1 must now be represented by the modified expression

$$p(\mathbf{x}) = \int_{\mathbf{\Omega}} p_{\mathrm{cn}}(\mathbf{x}|\sigma_n^2\mathbf{I}+\mathbf{R}_s)\, p(\mathbf{\Omega})\, d\mathbf{\Omega} \tag{10}$$

where $p(\mathbf{\Omega})$ is the (possibly multivariate) pdf for the vector of covariance-based random parameters.

The vector $\mathbf{\Omega}$ is defined to contain all unknown (random) parameters that affect the signal covariance. For example, in the trivial case that correlation and SNR are known, $\mathbf{\Omega}$ is simply an empty vector. For the case of fading with known correlation,

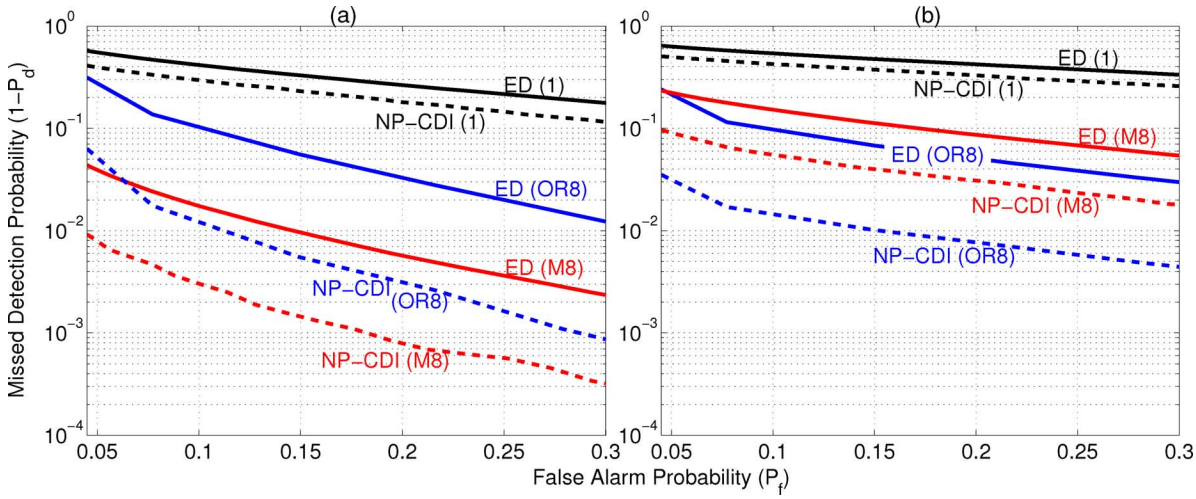

Fig. 3. Performance comparison of single-node and collaborative detection assuming error-free reporting channel: single sensor (1), eight-node OR fusion (OR8), eight-node majority fusion (M8) in (a) uniform real RCM in static sensing channel and (b) measured RCM in Rayleigh-fading sensing channel. Indicates a significant network-wide impact with CBD methods.

$\mathbf{\Omega} = [\sigma_s^2]$. In an extreme case, each element of the covariance matrix could be considered a separate random variable, such that $\mathbf{\Omega} = \mathrm{Vec}\{\mathbf{R}_s\}$, where $\mathrm{Vec}\{\cdot\}$ is the vector operation. Thus, the choice of $\mathbf{\Omega}$ depends on the modeling strategy and the knowledge available to the cognitive radio. In this work we consider a simple model where the random covariance is exponential, or

$$\phi_{s,k} = R_{s,i,i-k} = \sigma_s^2 |\rho_{s,1}|^{|k|} \exp(jk\angle\rho_{s,1}) \tag{11}$$

providing a three-parameter model $\mathbf{\Omega} = [\sigma_s^2 \;\; |\rho_{s,1}| \;\; \angle\rho_{s,1}]$ appropriate for this initial study.

Although $\sigma_s^2 = \sigma_n^2\gamma$ (γ is the SNR) is assumed to be fixed for a simple static channel model, we consider a few different models for $\rho_{s,1}$. The uniform correlation model assumes $|\rho_{s,1}| \sim U(0,1)$ with either zero phase $\angle\rho_{s,1} = 0$ (real correlation) or uniform phase $\angle\rho_{s,1} \sim U(0, 2\pi)$, which models the case where we expect correlation, but have no information about how it might be distributed. We also consider an RCM based on empirical distributions of $|\rho_{s,1}|$ and $\angle\rho_{s,1}$ obtained by direct spectrum measurements in the city of Bremen, which is described in Section IV. To obtain the detection performance based on the measured RCM, the channel is modeled to be Rayleigh-fading such that σ_s^2 (or equivalently γ for constant σ_n^2) is exponentially distributed, or

$$f(\gamma) = \frac{1}{\overline{\gamma}} \exp\left(-\frac{\gamma}{\overline{\gamma}}\right) \tag{12}$$

where $\overline{\gamma}$ is the average value of γ.

Computing the detection performance of the various CBD methods for an arbitrary RCM is complicated since $p(\mathbf{x};\mathsf{H}_1)$ can only be evaluated numerically. We adopt a Monte Carlo approach for computing performance, where the empirical distribution of the test statistic $\mathcal{T}(\mathbf{x})$ is found separately for hypotheses H_0 and H_1. For the case of H_0, M random noise vectors $\mathbf{x} = \mathbf{n}$ are generated and substituted into $\mathcal{T}(\mathbf{x})$ to obtain M random samples of $\mathcal{T}$. For the case of H_1, each realization requires $\mathbf{\Omega}$ (and hence $\mathbf{R}_s(\mathbf{\Omega})$) to be generated according to the RCM, a random waveform to be realized assuming $p(\mathbf{x}) = p_{\mathrm{cn}}(\mathbf{x}|\sigma_n^2\mathbf{I} + \mathbf{R}_s)$, after which $\mathcal{T}(\mathbf{x})$ is computed. From the M realizations of $\mathcal{T}(\mathbf{x})$ under H_0 and H_1, the distributions $p(\mathcal{T};\mathsf{H}_0)$ and $p(\mathcal{T};\mathsf{H}_1)$ are obtained, after which we can compute

$$P_{fa} = \int_{\mathcal{T}=\lambda}^{\infty} p(\mathcal{T};\mathsf{H}_0)\, d\mathcal{T} \tag{13}$$

$$P_d = \int_{\mathcal{T}=\lambda}^{\infty} p(\mathcal{T};\mathsf{H}_1)\, d\mathcal{T} \tag{14}$$

for arbitrary threshold λ.

When a closed form expression for P_d for a CBD method with fixed correlation is available, performance under the assumption of an RCM can be obtained using the average

$$P_d = \int_{\mathbf{\Omega}} P_d(\mathbf{\Omega})\, p(\mathbf{\Omega})\, d\mathbf{\Omega}. \tag{15}$$

For example, for the CorrSum method assuming fixed γ, $\angle\rho_{s,1} = 0$ and only $|\rho_{s,1}|$ is random, $P_d = \int_{|\rho_{s,1}|} P_d(|\rho_{s,1}|)\, p(|\rho_{s,1}|)\, d|\rho_{s,1}|$, where P_d as given by (37) in [10] is to be taken as $P_d(|\rho_{s,1}|)$.

B. Optimal Detection Methods (NP-PCI and NP-CDI)

First, we consider an optimal detector that has perfect correlation information (PCI) referred to as the NP-PCI detector. This assumes an adaptive sensing algorithm that somehow always knows $\mathbf{R}_s$ and σ_n^2. Although the NP-PCI detector is somewhat unrealistic for cognitive radio, it serves as a loose upperbound on performance and also indicates how much performance is gained by exactly knowing correlation as opposed to only knowing its distribution. Assuming a correlated complex Gaussian signal, where noise power σ_n^2 and signal covariance $\mathbf{R}_s$ are exactly known, the pdfs $p(\mathbf{x};\mathsf{H}_0)$ and $p(\mathbf{x};\mathsf{H}_1)$ are given by (9), and a sufficient test statistic for the NP detector is the so-called *estimator-correlator* , or

$$\mathcal{T}(\mathbf{x}) = \mathbf{x}^H\hat{\mathbf{s}} = \mathbf{x}^H\left[\mathbf{R}_s\left(\mathbf{R}_s + \sigma_n^2\mathbf{I}\right)^{-1}\mathbf{x}\right] \tag{16}$$

which corresponds to correlating the received waveform $\mathbf{x}$ with a Wiener filter estimate ($\hat{\mathbf{s}}$) of the signal $\mathbf{s}$. Evaluating P_{fa} and

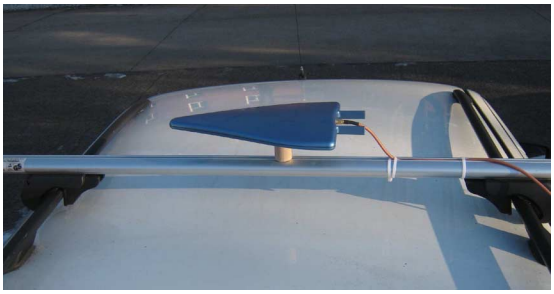

Fig. 4. Top view of the receive antenna mounted on the car used in the measurement campaign.

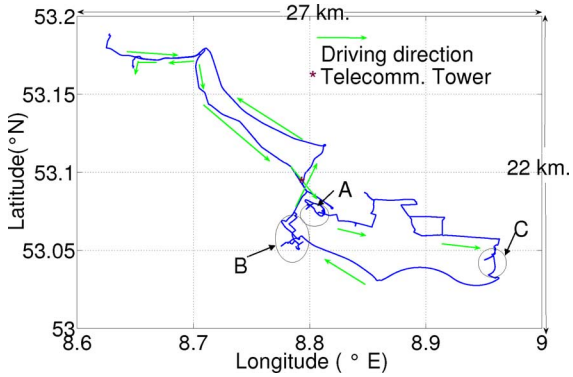

Fig. 5. The driving route during the measurement.

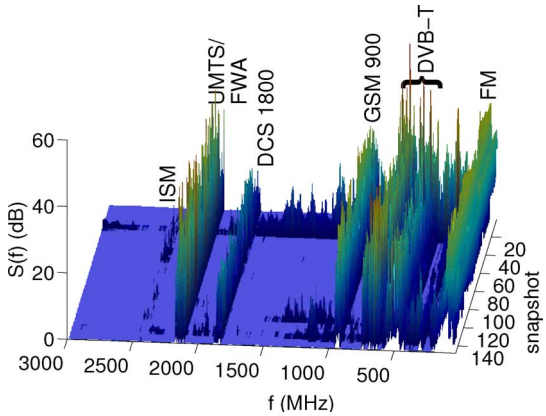

Fig. 6. Captured spectrum over the frequency range of 27 MHz to 3 GHz in dB relative to measured noise floor.

P_d require either Monte Carlo simulation or numerical evaluation of Fourier-type integrals [11].

A more practical upperbound for correlation based detection is possible by assuming that the cognitive radio has knowledge of the distribution of random correlation, but no knowledge of any particular realization of that process. We refer to this detector that optimally exploits correlation distribution information (CDI) as the NP-CDI detector. CDI is possible by considering what modulations and bandwidths may exist and with what likelihood in a particular band of interest. In this case, the optimal detector observes $\mathbf{x}$, forms $\mathcal{T}(\mathbf{x}) = \mathcal{L}(\mathbf{x})$ in (3), and compares to a threshold, where $p(\mathbf{x};\mathsf{H}_0) = p_{\mathrm{cn}}(\mathbf{x}|\sigma_n^2\mathbf{I})$ is computed in closed-form and $p(\mathbf{x};\mathsf{H}_1)$ is computed numerically using (10). By applying the above procedure in Monte Carlo simulations for M realizations of $\mathbf{x}$, the pdfs $p(\mathcal{L};\mathsf{H}_0)$ and $p(\mathcal{L};\mathsf{H}_1)$ are obtained and P_{fa} and P_d are computed using (13) and (14) with $\mathcal{T} = \mathcal{L}$.

IV. RCM Measurement Campaign

This section presents a measurement campaign that was performed to develop realistic RCMs, allowing us to judge the accuracy of the uniform correlation model and assess performance of CBD methods for practical scenarios.

A. Measurement System

Signal correlation in many bands was obtained by performing PSD measurements with a Rohde and Schwarz FSP7 spectrum analyzer in the 27 MHz to 7 GHz range. The antenna was a log-periodic antenna (HyperLOG 7060) with a nominal frequency range of 700 MHz to 6 GHz, horizontal polarization, and a fairly wide radiation pattern (5 dBi gain). Although the antenna had low efficiency (approximately 10 dB of additional loss) for frequencies below 700 MHz, we found that the FM and DVB-T signals of interest were sufficiently intense to be measured with high SNR using the antenna. The antenna was mounted on top of a car with the direction of maximum gain pointed perpendicular to the direction of travel, as depicted in Fig. 4. A global-positioning system (GPS) receiver was also available in the car, which was used to log position information over the entire measurement, allowing us to correlate our results with location. A laptop was used to both control the spectrum analyzer and log data during the measurement via a LAN interface. The laptop and spectrum analyzer were powered using a 12 V DC to 110 V AC power inverter.

To avoid influencing the measurements, the 802.11 card in the laptop was disabled and cellular telephones were turned off. The noise floor for each band was found by replacing the antenna with a terminator and performing a measurement. We also checked the interference imposed by the inverter and/or car by running the equipment in a stationary car either with the inverter (car ON) or a long extension cord (car ON and OFF). We found that the running car alone had little effect on the bands of interest, but that the inverter did cause some small additional interference at the lower frequency bands, but insufficient to change any results.

B. Measurement Scenario

Measurements were performed in and around the city of Bremen, Germany, and the driving path reconstructed from GPS data is shown in Fig. 5. Many snapshots of all the spectrum bands were obtained by driving for approximately 3 h along the route. More time was spent in the highlighted areas A (downtown Bremen), B (near airport), and C (shopping mall), since more RF activity was expected to be present. Signals of interest were identified using the frequency assignment information for Germany found in [19], provided by the German Bundesnetzagentur.

Fig. 6 Depicts the PSD measurements for the whole driving track, where activity in FM (87.5–108 MHz), DVB-T (3 channels in 470–606 MHz band and four channels in 614–790 MHz band), GSM-900, DCS-1800, fixed wireless access (FWA) and UMTS downlink (2110–2170 MHz), and ISM (2400–2483.5 MHz) bands is evident. Significant white spaces are also seen in the spectrum. Spectrum in the 3–7 GHz range

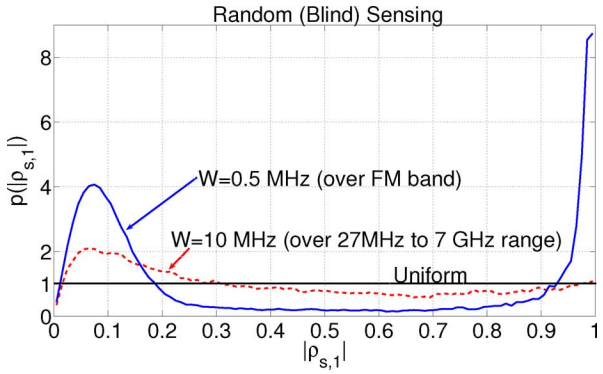

Fig. 7. Correlation magnitude pdf of $|\rho_{s,1}|$ for random sensing.

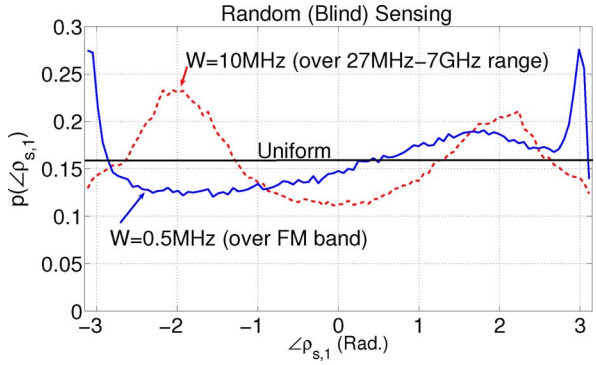

Fig. 8. Measured pdf of $\angle\rho_{s,1}$ for random sensing.

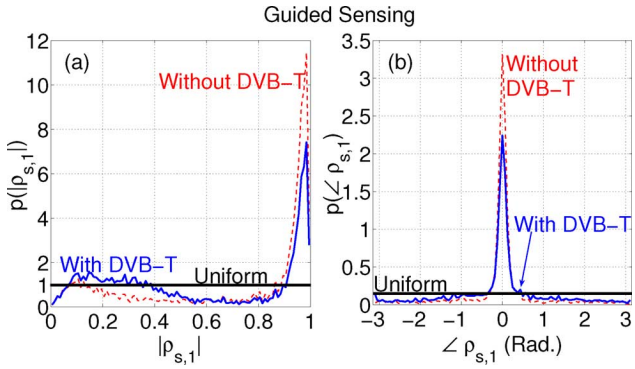

Fig. 9. Measured pdfs of $\rho_{s,1}$ for guided sensing: (a) magnitude and (b) phase.

was only occupied in a few isolated cases: 3400–3475 MHz (near the Telecomm tower), 5230–5250 MHz (near the airport), 4610 MHz (military band sporadically present), and 5685–5690 MHz (single snapshot near downtown). The apparent horizontal lines in spectrum near snapshots 26 and 110 occurred when the receiver was near the Telecomm tower, where extensive RF activity was present.

C. Measurement-Based RCM

Measured PSD data was analyzed to obtain the distribution of the correlation for a sensing bandwidth W in two different ways: (i) guided sensing where correlation is computed using spectrum centered at known carrier frequencies and (ii) random (blind) sensing where bandwidth W about a randomly (uniform) selected center frequency is taken. In both cases only spectrum that was at least partially occupied (signal 5 dB above the noise floor was present) within the sensing bandwidth was used as a correlation sample for the RCM. Choosing guided or random sensing is expected to have a significant impact on CBD methods, since in the former case correlation is real, while in the latter it is likely to have uniform phase. The PSD in sensing bandwidth W is converted to correlation by shifting to baseband, performing an inverse Fourier transform, and normalizing to obtain $\rho_{s,k}$.

The pdf of $|\rho_{s,1}|$ for random sensing obtained from the measurement data is shown in Fig. 7, where sensing in the FM bands with $W = 500$ kHz yields a bimodal distribution with peaks near 1 and 0.07. For the case of larger W and random sensing in the full spectrum, the pdf is flatter with a small peak at low correlation and no peak near $|\rho_{s,1}| = 1$. The pdf of phase $\angle\rho_{s,1}$ for random sensing is given in Fig. 8, which is similar to a uniform distribution.

Fig. 9 plots the case of guided sensing for the full spectrum, where for each center frequency W is chosen to be equal to the known channel bandwidth. Additionally, cases of DVB-T being included or excluded are considered to check the impact of very flat (uncorrelated) transmissions. Correlation magnitude has a sharp peak for high correlation as well as significant support at low correlation values, which is largely due to the DVB-T bands. As expected, correlation phase is nearly zero for known carrier frequencies.

V. Performance Assessment

Having developed the framework for random correlation modeling, this section gives numerical examples of performance upperbounds and the performance of ad-hoc methods, indicating where correlation-based detectors are advantageous.

A. Upperbounds: NP-PCI and NP-CDI

Here we consider the NP-PCI and NP-CDI bounds applied to the uniform RCM, indicating the maximum performance improvement that is available for methods that exploit signal correlation. We also consider how robust theoretical detection performance is in the presence of error in the estimated SNR.

1) Bounds for Guided Sensing: Fig. 10 presents detection performance of ED, NP-PCI, and NP-CDI for guided sensing, where $|\rho_{s,1}| \sim U(0,1)$ and $\angle\rho_{s,1} = 0$. The bottom bar groups show that CDI provides a 10%–20% performance improvement compared to ED. Encouragingly, detection performance of NP-CDI is only about 5%–10% less than NP-PCI, suggesting that a large fraction of the potential benefit from correlation can be captured with distribution knowledge.

Since SNR is a parameter used in both the NP-PCI and NP-CDI detectors, the upper four bar groups in Fig. 10 indicate the loss in detection performance when an incorrect assumption about this parameter is made, where negative (-12 dB) and positive ($+12$ dB) error is considered. We note that although NP-CDI is fairly robust to both positive and negative SNR error, the NP-PCI detector loses significant performance when SNR is overestimated. Although not plotted, results for the

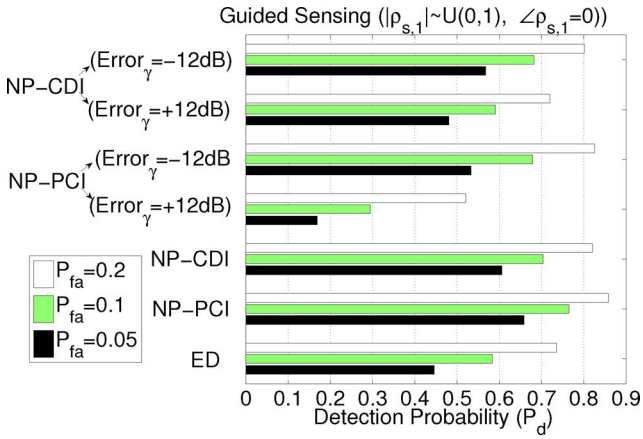

Fig. 10. Bounds for guided sensing (real correlation) under uniform RCM.

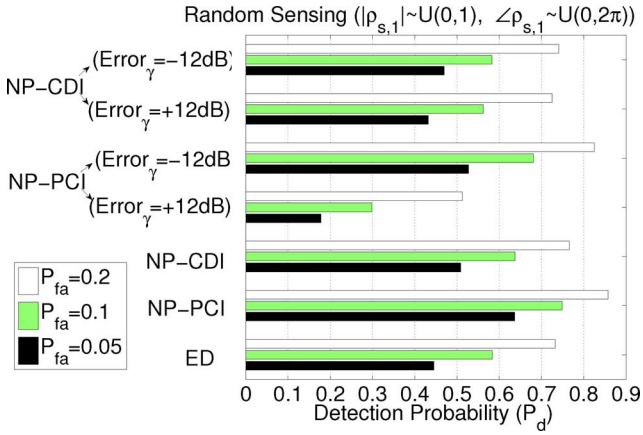

Fig. 11. Performance comparison for random sensing (complex autocorrelation) for CDI under uniform RCM.

measurement based RCM with guided sensing are similar to this zero-phase uniform correlation model case.

2) Bounds for Random Sensing: Next, Fig. 11 considers random sensing $|\rho_{s,1}| \sim U(0,1), \angle\rho_{s,1} \sim U(0,2\pi)$. Although NP-PCI still provides a 10%–20% improvement in detection performance, NP-CDI provides very little improvement (3%–6%), indicating that exploiting correlation for unknown transmission center frequency is not very fruitful.

B. Performance of CAV and CorrSum

This section studies several important aspects of the ad-hoc methods (CAV and CorrSum) using the developed RCMs.

1) Constant Correlation Versus Random Correlation: Fig. 12 explores the difference of having a fixed correlation $\rho_{s,1} = 0.5$ versus random uniform correlation $\rho_{s,1} \sim U(0,1)$ for guided sensing $\angle\rho_{s,1} = 0$. We see that the performance of CorrSum and CAV for the RCM is very similar to the performance for a fixed correlation at the mean value, suggesting that a rough estimate of performance is possible by just using the average expected correlation value, rather than very detailed RCM simulations. We also observe that using an additional lag ($L = 3$) has very little impact on performance. Although CorrSum has higher performance than CAV due to the reasons

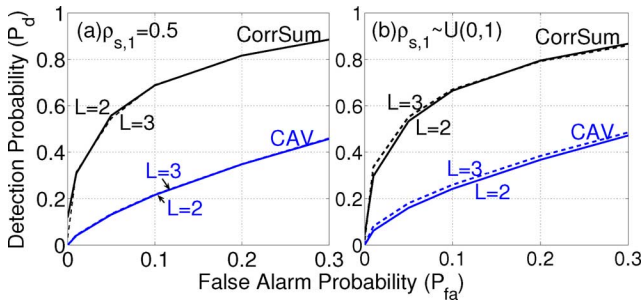

Fig. 12. Comparison of ad-hoc CBD methods for (a) constant correlation and (b) random correlation assuming a simple uniform RCM.

explained in Section II-C, we have found that if the trace normalization in (6) is removed, CAV has performance near ED.

2) Real Versus Complex Autocorrelation: Fig. 13 compares real autocorrelation (guided sensing) to the case of complex autocorrelation (random sensing) for the uniform correlation model and an optimal value of $L = 2$, where energy detection has also been considered for comparison. CAV performance is insensitive to nonzero phase, but CorrSum performance suffers and drops below ED. It is also interesting that the NP-CDI bound indicates that around 7% performance improvement relative to the best practical method is still possible.

3) Effect of Noise Uncertainty: Noise uncertainty of the various detection methods is analyzed using the approach from [16]. Here, the noise variance under NU is $\sigma_{nu}^2 \in [(1/\Phi)\sigma_n^2, \Phi\sigma_n^2]$, where Φ is the uncertainty factor expressed in dB, and robust sensing assumes $\sigma_{nu}^2 = \Phi\sigma_n^2$ and $\sigma_{nu}^2 = (1/\Phi)\sigma_n^2$ under H_0 and H_1, respectively. The SNR wall [16] is the SNR below which $P_d < P_{fa}$ and for $\Phi = 0.1$ dB the SNR wall for ED and CorrSum ($\rho_{s,1} = 0.5$) are found to be -13.4 dB and -15.1 dB, respectively. Similarly, the SNR wall for NP-CDI for real uniform RCM and $P_{fa} = 0.2$ is found to be -17 dB. Note that SNR wall does not exist for CAV.

Fig. 13(a) plots the effect of NU for the real correlation scenario, where NU degrades the performance (with increasing severity) of NP-CDI, CorrSum, and ED, while CAV performance remains unchanged. With increasing Φ, ED degrades to the performance of CAV at $\Phi = 0.17$ dB, followed by CorrSum at $\Phi = 0.275$ dB. Also shown is that the SNR wall for ED and CorrSum is -9 dB (the simulated SNR) for $\Phi = 0.275$ dB and $\Phi = 0.41$ dB, respectively. Although not plotted to reduce clutter, NP-CDI performance for $P_{fa} = 0.2$ reaches the -9 dB SNR wall for a noise uncertainty of 0.52 dB. Similarly for complex correlation in Fig. 13(b), CorrSum and NP-CDI are degraded by NU, where CorrSum performance degrades to CAV at $\Phi = 0.17$ dB and fails near $\Phi = 0.275$ dB. Note that NP-CDI performance for $P_{fa} = 0.2$ reaches the -9 dB SNR wall for a noise uncertainty of 0.35 dB.

4) Experimental RCM With Guided Sensing: Fig. 14 now considers guided sensing in a Rayleigh fading environment for RCMs that were derived from the measurement, where we exclude or include the DVB-T bands. Including DVB-T transmissions reduces the performance of both the CorrSum and CAV methods, as well as the NP-CDI bound, due to reduced correlation from these flat noise-like OFDM transmissions. CorrSum

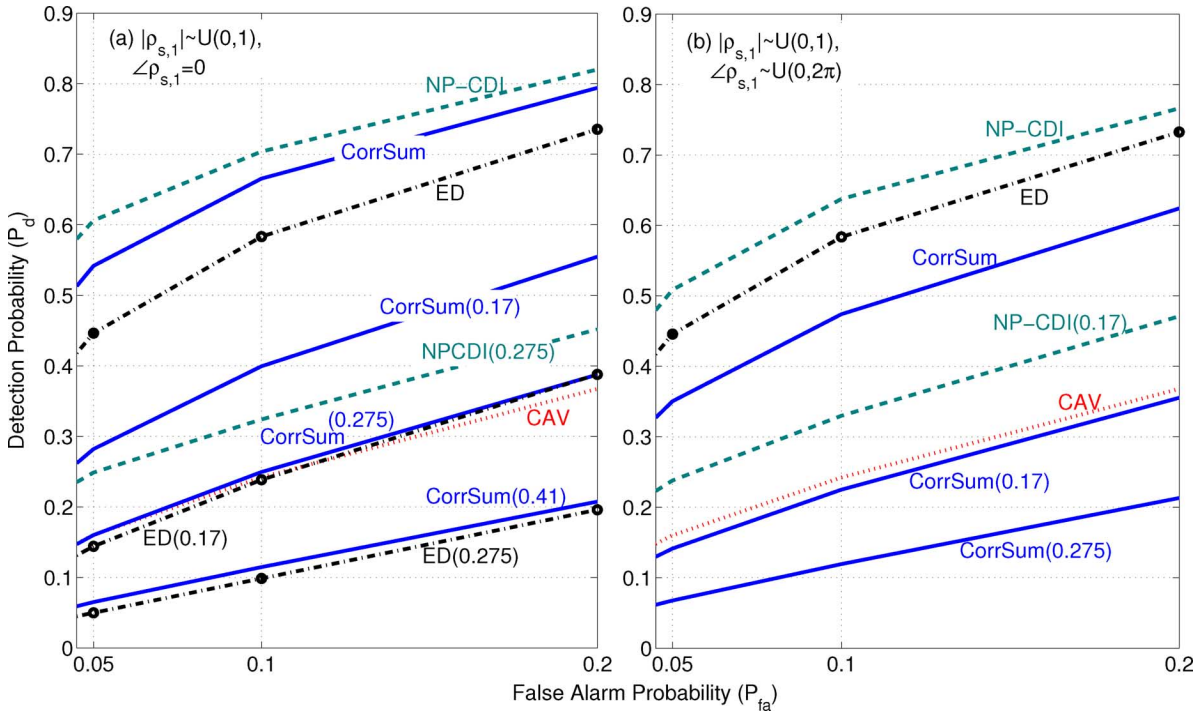

Fig. 13. Comparison of ad-hoc CBD methods for (a) real autocorrelation (guided) and (b) complex autocorrelation (random) sensing. The number inside the parenthesis for each method is the NU (Φ) in dB.

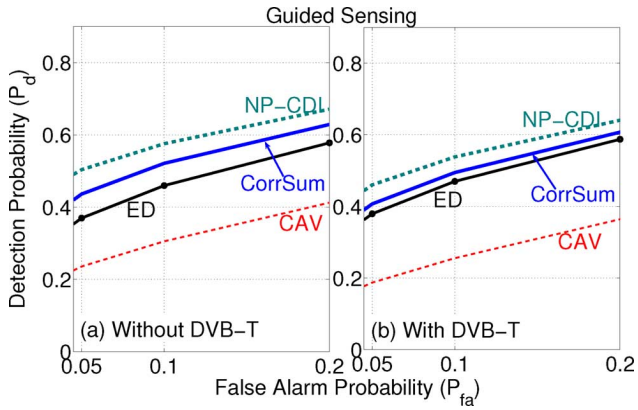

Fig. 14. Performance of guided ad-hoc CBD methods computed using experimental RCMs and Rayleigh-fading, where noise-like DVB-T transmissions are (a) excluded or (b) included in the model.

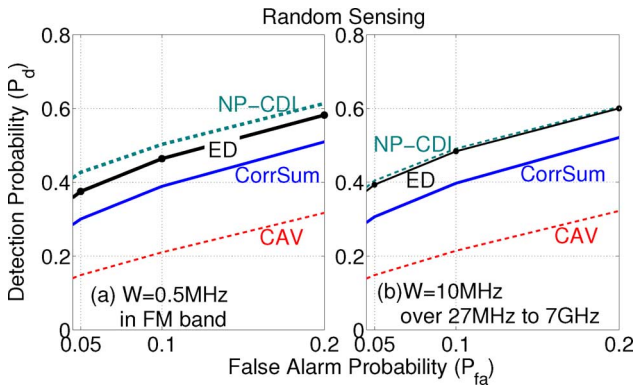

Fig. 15. Performance of ad-hoc CBD methods computed using experimental RCMs and Rayleigh-fading for random sensing: (a) only FM bands, (b) entire 27 MHz–7 GHz spectrum.

detection is about 10% better than ED without DVB-T, but only about 4% better when DVB-T transmissions are included. In both cases, the NP-CDI bound indicates that significant improvements are still possible.

5) Experimental RCM With Random Sensing: Fig. 15 considers the same experimental RCM in Rayleigh-fading, but now for the case of random (blind) sensing. On the left, sensing with $W = 500\,\mathrm{kHz}$ in the FM bands only is considered, while on the right $W = 10\,\mathrm{MHz}$ for the whole spectrum (27 MHz–7 GHz) is considered. The basic result is that CorrSum performance is degraded and is lower than ED. Also, the NP-CDI bound indicates that although slight performance improvement with CBD relative to ED is possible in the FM bands, negligible improvement is possible when the whole spectrum is considered.

VI. Conclusion

Correlation-based detection has been identified as a method for increasing performance and robustness of primary user detection in cognitive radio networks. This work has provided a rigorous framework for studying the performance of correlation-based detectors by introducing the concept of random correlation models (RCMs). A measurement campaign was presented where spectral measurements in Bremen, Germany, were taken, demonstrating how realistic RCMs can be derived. This effort also led to the natural development of an NP detector that exploits correlation distribution information (CDI) as opposed to the instantaneous correlation, which is not expected to be known by uninformed cognitive radios. The NP-CDI performance serves as the upperbound on the performance of all methods that exploit signal autocorrelation.

Subsequent analysis indicated that the main improvements with correlation-based detection are available when the transmission center frequencies are known (guided sensing). For completely blind sensing, methods that exploit only real correlation (like CorrSum) are degraded, and methods that ignore correlation phase (like CAV) are unaffected. In many cases, however, the NP-CDI bound exhibited higher performance than the existing methods, even in the case of blind sensing, indicating that some improvement in the ad-hoc sensing methods is still possible.

REFERENCES

[1] J. Mitola, III and G. Q. Maguire, Jr., "Cognitive radio: Making software radios more personal," *IEEE Personal Commun. Mag.*, vol. 6, pp. 13–18, Aug. 1999.

[2] T. Yücek, "Spectrum sensing for cognitive radio applications," in *Cognitive Radio, Software Defined Radio, and Adaptive Wireless Systems*, H. Arslan, Ed. New York: Springer, 2007, ch. 9.

[3] A. Ghasemi and E. Sousa, "Asymptotic performance of collaborative spectrum sensing under correlated log-normal shadowing," *IEEE Commun. Lett.*, vol. 11, no. 1, pp. 34–36, Jan. 2007.

[4] M. Renzo, L. Imbriglio, F. Graziosi, and F. Santucci, "Distributed data fusion over correlated log-normal sensing and reporting channels: Application to cognitive radio networks," *IEEE Trans. Wireless Commun.*, vol. 8, pp. 5813–5821, Dec. 2009.

[5] K. Ben Letaief and W. Zhang, "Cooperative communications for cognitive radio networks," *Proc. IEEE*, vol. 97, pp. 878–893, May 2009.

[6] H. Urkowitz, "Energy detection of unknown deterministic signals," *Proc. IEEE*, vol. 55, pp. 523–531, Apr. 1967.

[7] V. I. Kostylev, "Energy detection of a signal with random amplitude," in *Proc. 2002 IEEE Int. Conf. Commun.*, Apr. 2002, vol. 3, pp. 1606–1610.

[8] F. F. Digham, M. Alouini, and M. K. Simon, "On the energy detection of unknown signals over fading channels," in *Proc. 2003 IEEE Int. Conf. Commun.*, May 2003, pp. 3575–3579.

[9] Y. Zeng and Y.-C. Liang, "Spectrum-sensing algorithms for cognitive radio based on statistical covariances," *IEEE Trans. Veh. Technol.*, vol. 58, no. 4, pp. 1804–1815, May 2009.

[10] R. K. Sharma and J. W. Wallace, "Improved spectrum sensing by utilizing signal autocorrelation," in *Proc. 2009 IEEE 69th Veh. Technol. Conf.*, Barcelona, Spain, Apr. 2009, pp. 1–5.

[11] S. M. Kay, *Fundamentals of Statistical Signal Processing: Detection Theory*. Englewood Cliffs, NJ: Prentice-Hall, 1998, vol. II.

[12] W. Gardner, "Exploitation of spectral redundancy in cyclostationary signals," *IEEE Signal Process. Mag.*, vol. 8, no. 2, pp. 14–36, Apr. 1991.

[13] R. S. Roberts, W. A. Brown, and H. H. Loomis, Jr., "Computationally efficient algorithms for cyclic spectral analysis," *IEEE Signal Process. Mag.*, vol. 8, no. 2, pp. 38–49, Apr. 1991.

[14] D. Cabric, "Addressing feasibility of cognitive radios," *IEEE Signal Process. Mag.*, vol. 25, no. 6, pp. 85–93, Nov. 2008.

[15] I. Akyildiz, W.-Y. Lee, M. Vuran, and S. Mohanty, "A survey on spectrum management in cognitive radio networks," *IEEE Commun. Mag.*, vol. 46, pp. 40–48, Apr. 2008.

[16] R. Tandra and A. Sahai, "SNR walls for signal detection," *IEEE J. Sel. Topics Signal Process.*, vol. 2, pp. 4–17, Feb. 2008.

[17] R. K. Sharma and J. W. Wallace, "A novel correlation sum method for cognitive radio spectrum sensing," in *Proc. 2008 URSI XXIXth Gen. Assembly*, Chicago, IL, Aug. 2008.

[18] Z. Chair and P. K. Varshney, "Optimal data fusion in multiple sensor detection systems," *IEEE Trans. Aerosp. Electron. Syst.*, vol. 22, pp. 98–101, Jan. 1986.

[19] Frequenznutzungsplan. Deutschland, Bundesnetzagentur, Apr. 2008. [Online]. Available: http://www.bundesnetzagentur.de/media/archive/17448.pdf

Rajesh K. Sharma (S'07) received the B.Sc. degree (with honors) in electrical engineering from the University of Engineering and Technology (UET), Lahore, Pakistan, in 1998 and the M.Eng. degree in telecommunications from the Asian Institute of Technology (AIT), Thailand, in 2002. He is currently working towards the Ph.D. degree at the School of Engineering and Science, Jacobs University, Bremen, Germany, since 2007.

During his B.Sc. and M.Eng. studies, he was supported by scholarships from the government of Pakistan and the government of Finland, respectively. From 1999 to 2001, he worked as a Lecturer and from 2003 to 2007 as an Assistant Professor, both in the Department of Electrical and Electronics Engineering, Kathmandu University, Nepal. His current research interests include cognitive radio, MIMO communications, wireless physical layer security, and wireless channel modeling.

Jon W. Wallace (S'99–M'03) received the B.S. (*summa cum laude*) and Ph.D. degrees in electrical engineering from Brigham Young University (BYU), Provo, UT, in 1997 and 2002, respectively.

From 1995 to 1997, he worked as an associate of Novell, Inc., Provo, UT, and during 1997, he was a Member of Technical Staff for Lucent Technologies, Denver, CO. He received the National Science Foundation Graduate Fellowship in 1998 and worked as a Graduate Research Assistant at BYU until 2002. From 2002 to 2003, he was with the Mobile Communications Group, Vienna University of Technology, Vienna, Austria. From 2003 to 2006, he was a Research Associate with the BYU Wireless Communications Laboratory. Since 2006, he has been an Assistant Professor of Electrical Engineering at Jacobs University, Bremen, Germany. His current research interests include wireless channel sounding and modeling, wireless security, MIMO communications, cognitive radio, and UWB systems.

Dr. Wallace is an Associate Editor of the IEEE TRANSACTIONS ON ANTENNAS AND PROPAGATION.